Strong Electronic Communication in Linearly Elongated Rylenes Featuring Tunable Bridges

Michaela Dobeneck,[a] Ramandeep Kaur,[b] Benedikt Platzer,[b] Dirk M. Guldi,*[b] and Andreas Hirsch*[a]

Abstract: A modified synthetic pathway towards perylene-perylene dimers and a facile purification method to obtain the regioisomerically pure *syn*- and *anti*-isomers are reported. In addition, a novel perylene-naphthalene heterodimer with 30 conjugated π-electron pairs was designed and synthesized on the basis of a previously described precursor and the resulting regioisomers were separated from each other. Thereby, the opto-electronic properties of the linearly elongated chromophores could be investigated regarding the differences in length of their aromatic system and the configuration of the isomers. Further tuning of their energy gaps was realized *via* protonation and methylation of the dibenzimidazole-bridging unit. Extraordinary red-shifts of the absorption maxima of 62 nm for the methylated and 92 nm for the protonated perylene-perylene *anti*-isomer could be achieved. Moreover, the maxima for the *syn*-isomer could be shifted bathochromically by 87 and 113 nm, respectively.

Introduction

Colors have always been part of human life. Therefore, the synthetic manufacturing of colorants is very important and one of the most explored areas in industrial organic chemistry. Rylene-based pigments (insoluble) and dyes (soluble) have attracted great attention in the academic and industrial fields of dyestuff chemistry, since they are not only very good colorants, but they also possess high chemical, thermal, and photochemical stability.[1] Rylene-bis(dicarboximides) are based on a linear connection of naphthalene units between two terminating imide groups (Figure 1). The smallest representatives of this homologous series are naphthalenebis(dicarboximides) (NBIs, $n=0$)[2] followed by perylenebis(dicarboximides) (PBIs, $n=1$)[1b,3] as the most important member of the family up to octarylene-(dicarboximide)s (OBIs; $n=7$)[4] as the largest ones.

This extension of the aromatic system goes hand in hand with a stepwise bathochromic shift of the absorption and emission bands within the rylene family.[1a] Whereas the smaller

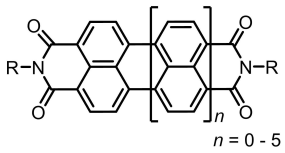

Figure 1. General construction principle of rylene-bis(dicarboximide)s.

PBIs have absorption maxima at $\lambda_{max} \approx 520$ nm[1b,5], those for the longest homologues, the OBIs, appear in the near-infrared region at $\lambda_{max} = 1007$ nm[4]. However, the enlargement of the rylenes π-system results in a significant reduction of the higher order chromophores solubility and processability.[1a,6]

As compared to other organic dyes, PBIs provide a manifold of functionalization opportunities transferring them from insoluble pigments to soluble dyes and to further tune their optical properties, emphasizing their role as the most extensively studied representatives of this class of dyes.[1a,3a,7] Structural modifications *via* variation of the nature and the position of substituents at the perylene core offer access to many tailored functional chromophores. In both, research and industry, perylene-3,4,9,10-tetracarboxylic dianhydride (PTCDA, $n=1$, Figure 2) is the primary starting material for the synthesis of PBIs.

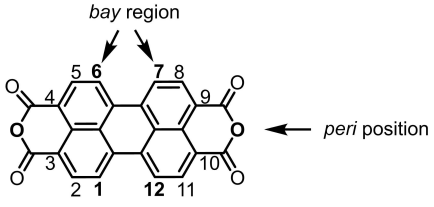

Figure 2. Illustration of the *bay* and *peri* positions in perylene-3,4,9,10-tetracarboxylic dianhydride.

[a] M. Dobeneck, Prof. Dr. A. Hirsch
Department of Chemistry and Pharmacy
Friedrich-Alexander-University Erlangen-Nuremberg
Organic Chemistry II, Nikolaus-Fiebiger-Str. 10, 91058 Erlangen (Germany)
E-mail: andreas.hirsch@fau.de

[b] R. Kaur, B. Platzer, Prof. Dr. D. M. Guldi
Department of Chemistry and Pharmacy
Friedrich-Alexander-University Erlangen-Nuremberg
Physical Chemistry I, Egerlandstr. 3, 91058 Erlangen (Germany)
E-mail: dirk.guldi@fau.de

Supporting information for this article is available on the WWW under https://doi.org/10.1002/chem.202005335

Imidization of the dianhydride with long-chain alkyl- or arylamines in *peri* position leads to the corresponding PBI or perylene monoimide monoanhydride (PMI) compounds with reasonable solubility.[1b,3a,8] The introduction of bulky substituents in the *bay* (1,6,7,12) region causes introduction of steric strain in the molecule and twisting of the two naphthalene half units out of planarity.[1b,5] In this way, introduction of substituents not only improves the solubility, but also alters the electronic and optical properties of the chromophore.

Further color tuning can be provided *via* the condensation of aromatic units to the *peri* positions of perylene dianhydride (PDA) or PMI. First, only small molecules like *o*-diaminobenzene were connected to the perylenes[9], but the anhydride-amine condensation presented the possibility to attach also larger aromatic units[9a]. Recently, this condensation concept was used to synthesize linear architectures with up to 35 conjugated π-electron pairs *via* the connection of two perylene monoimides by means of a 1,2,4,5-benzenetetraamine bridge. Thereby, perylene homodimers in *anti*- (**I**) or *syn*- (**II**) configuration were obtained.[10] (Figure 3)

We have recently reported on a mixture of the long-wavelength-absorbing homodimers with reasonable solubility.[11] For this purpose, sterically demanding *t*-butyl-phenoxy-groups were added in the *bay* regions of the perylenes. The absorption maximum at $\lambda_{max} = 650$ nm could be shifted *via* protonation of the bridging unit with TFA to $\lambda_{max} = 773$ nm. This is comparable to the maximum absorption of bay-substituted quaterrylenebis-(dicarboximide)s (QBI, $n = 3$) at 764 nm.[12]

More recently, we have extended the group of linearly elongated perylene dyes from homodimeric structures towards heterodimeric perylene-diketones **3** (Scheme 1).[13] The synthetic pathway started from a novel precursor **1** that was connected with several *ortho*-diketones **2**. The step-by-step synthesis enabled the facile access to a library of expanded perylene dyes without the formation of homodimeric by-products. The absorption maxima of the heterodimers were bathochromically shifted by up to 40 nm compared to PBI references.

These different examples show the great potential of perylene dyes to tune their HOMO-LUMO gaps (HOMO = highest occupied molecular orbital, LUMO = lowest unoccupied molecular orbital) *via* linear elongation of their aromatic system. Thereby many stable chromophores with reasonable solubility could be created. However, all the homodimeric perylene chromophores reported before were characterized as mixtures of their *syn*-and *anti*-configurations. This complicates the determination of structure-property relationships of the dimers.[14] In this study, we present a modified synthetic pathway towards perylene-perylene homodimers and a purification method to separate their *anti*- from *syn*-isomers.

To compare not only the difference of the configuration on the optical and electrochemical properties but also the effect of the π-systems size, we synthesized and characterized novel heterodimeric perylene-naphthalene dimers **4** and **5** (Figure 4) with 30 conjugated π-electron pairs on the basis of previously reported precursor **1**.

Furthermore, we found a facile way to further tune the HOMO-LUMO gaps of the linearly elongated perylene homo- and heterodimers *via* modification of their bridging units.

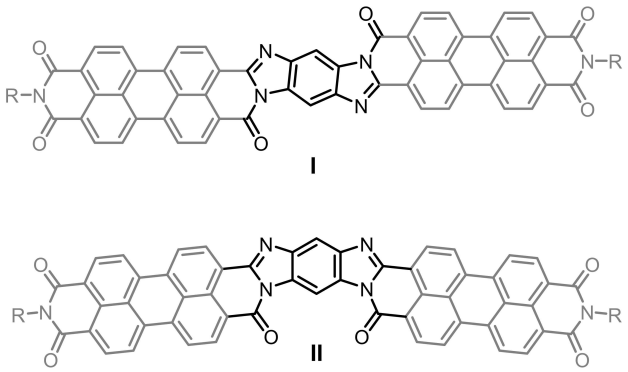

Figure 3. *Anti*- (**I**) and *syn*- (**II**) configurations of a perylene-perylene-dimer.[10,11]

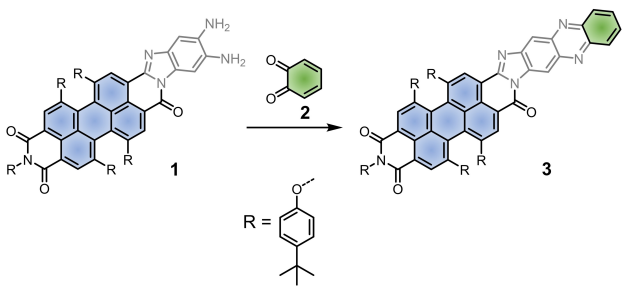

Scheme 1. Reaction of perylene precursor **1** with *o*-diketones (for example 1,2-benzoquinone **2**) towards heterodimeric perylene-diketones **3**.[13]

Results and Discussion

Perylene-perylene dimers

The synthesis of the linearly elongated perylene compounds **8** and **9** was carried out starting from tetra-*bay*-substituted PMI **6** (Scheme 2) that was obtained *via* modified literature procedures.[15] The long, branched alkyl chains in *peri* position

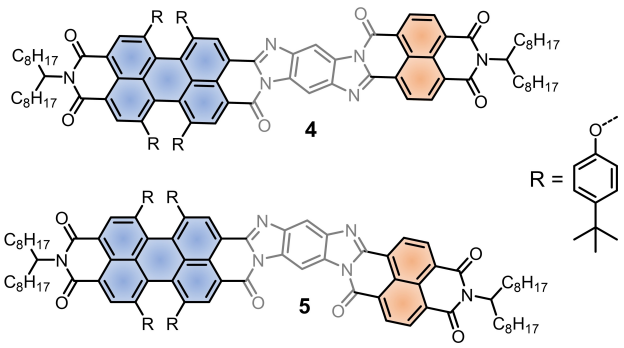

Figure 4. *Anti*- (**4**) and *syn*- (**5**) isomers of perylene-naphthalene-hybrids.

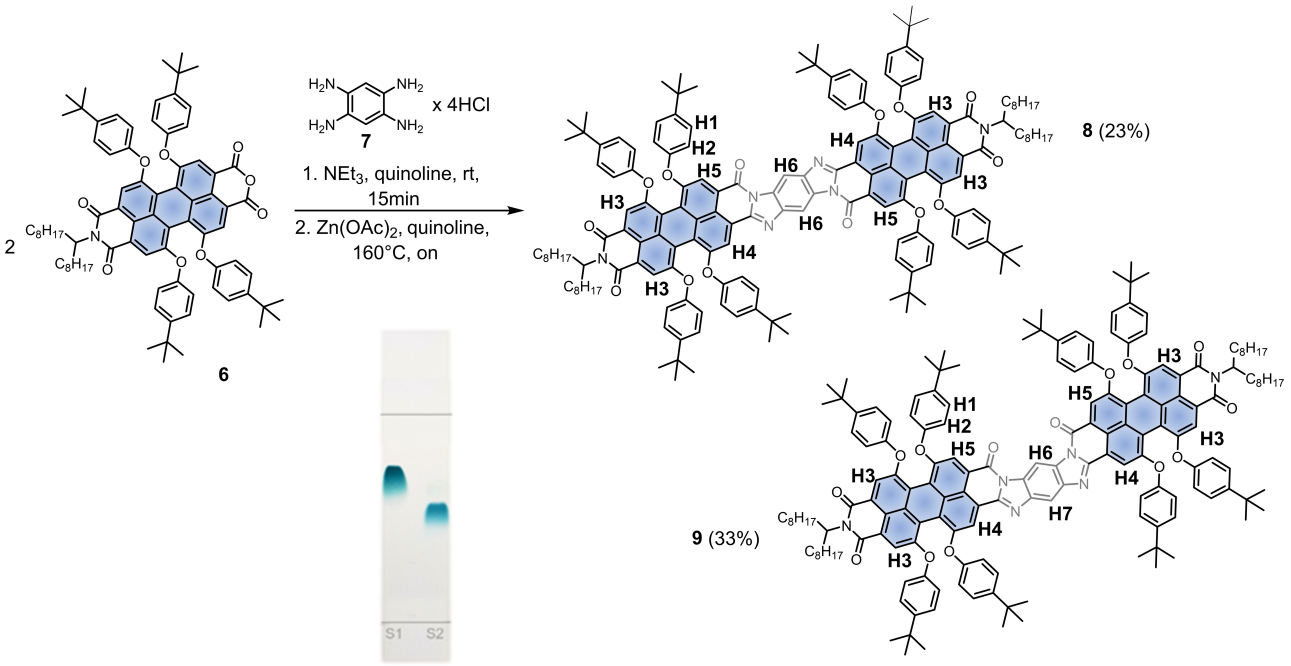

Scheme 2. Condensation of tetra-*bay*-substituted PMI **6** with 1,2,3,4-tetraminobenzene **7** towards the *anti*- and *syn*-isomers **8** and **9** of perylene-perylene dimer Inset: picture of the newly separated sample on a TLC-SiO_2 plate (CH_2Cl_2:*n*-hexane 1:1).

and the sterically demanding *t*-butyl-phenoxy groups in the *bay*-region guarantee reasonable solubility in many solvents.[1b,3a,5,8] Two equivalents of PMI **6** were condensed with 1,2,4,5-tetraminobenzene **7** in freshly distilled and degassed quinoline under inert conditions. The unstable tetra-amino compound **7** was formed *in situ* before the condensation from its tetrahydrochloride and triethylamine. Starting the synthetic pathway from the monoimide monoanhydride compound instead of the dianhydride prevents the condensation to longer oligomers as by-products and, thereby, results in easier purification procedures. Simple plug chromatography on silica gel (CH_2Cl_2:hexanes 3:7→1:1) led to the removal of impurities and allowed for the separation of the constitutional isomers. The green *anti*-compound **8** (Rf = 0.7) was obtained in 23% and the dark blue dimer with *syn*-configuration (**9**, Rf = 0.5) in 33% yield.

The underlying colour change from pink (**6**) to blue (**8**) and green (**9**) suggested the success of the reaction. The reaction products were fully characterized. High resolution mass spectrometry [MALDI-TOF MS or ESI/atmospheric pressure photoionization (ESI/APPI)] proofed the expected composition.

Based on the aromatic regions of the proton NMR spectra depicted in Figure 5, it was possible to distinguish between the *anti*- and the *syn*-isomer **8** and **9**. Both chromophores show two multiplets in the range between 7.27 and 6.82 ppm representing the 16 aromatic protons H1 and H2 of the *bay* substituents. Another similarity are the signals for the perylene protons H3–H5. An exact assignment of these hydrogens was possible with the help of HMBC spectra (Heteronuclear Multiple Bond Correlation, see Supporting Information). A relation between H3 and the alkyl chains assigns the singlets at δ = 8.20 and

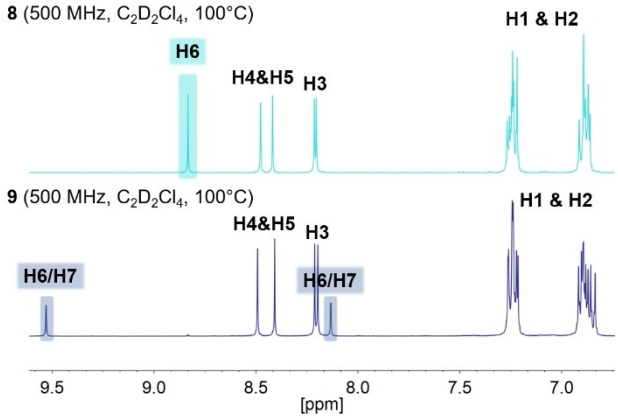

Figure 5. Aromatic regions of *anti*- and *syn*-isomers **8** and **9**. For the assignment of signals see Scheme 2.

8.19 ppm to be the outer perylene protons that are less affected by the *syn*/*anti*-isomerism.

However, the signals for H4 and H5 differ significantly in terms of their shifts based on their different chemical surroundings at the benzimidazole bridge. Of most importance are the signals of the bridging units. Due to symmetry reasons, the *anti*-configuration of the dimer displays only one signal H6 for the bridging unit at δ = 8.83 ppm. This assignment is based on the lack of a cross-peak in the HMBC spectrum of **8**. The *syn*-isomer shows two duplets H6 and H7 at δ = 9.52 and 8.13 ppm with a coupling constant J = 0.8 Hz for the bridging unit.

Steady-state absorption and fluorescence of perylene-perylene homodimers

Absorption and fluorescence spectra of perylene-perylene dimers **8** and **9** were recorded in toluene, anisole, and benzonitrile – Figures 6, S11, and S12. The spectra are separated into the spectral regions from 320 to 500 nm and from 500 to 700 nm. In the earlier, maxima are noted around 327, 400, and 450 nm, while in the latter maxima evolve at 624 and 657 nm for **8** and at 567 and 609 nm for **9**. Overall, the absorption spectrum of **9** compares well with that of heterodimer **3**[13] with maxima at 572 and 617 nm. **8**, in contrast, is notably red-shifted.

Appreciable red-shifts occur for both homodimers in more polar solvents. The fluorescence mirror-images the absorption. Here, maxima are at 679 and 640 nm for **8** and **9**, respectively. Considering the long-wavelength absorption and the short-wavelength fluorescence, HOMO-LUMO gaps of 1.86, 1.97 and 1.97 eV were calculated for **8**, **9**, and **3**, respectively. Fluorescence quantum yields Φ_{Fl}, which were determined vs. Rhodamine B in ethanol, are generally high in toluene with 0.13 (**8**) and 0.47 (**9**) and, in turn, similar to that for **3** with 0.26.[16] The quantum yields drop, however, below 0.01 when using more polar solvents (Table 1).

Electrochemistry of perylene-perylene homodimers

Differential pulse voltammograms (DPVs) and cyclic voltammograms (CVs) were recorded in CH_2Cl_2 with $[NBu_4][PF_6]$ as electrolyte, using a three-electrode system. Combination of the two methods helped to resolve overlapping electrochemical processes and to study their reversibility. Recorded potentials were corrected against an internal reference, i.e. Fc/Fc^+ redox couple. We compared the two enantiomers (*anti* and *syn*) of homodimers **8** and **9** with the heterodimer **3**. In contrast to **3**, **8** and **9** both exhibit partly overlapping and closely occurring oxidations and reductions corresponding to the two perylenes in the homodimers. (Figures S13-16, and Table 2). This is indicative for strong inter-perylene interactions. For example in **8**, the first reversible oxidation includes two one-electron oxidations at +0.79 and +0.89 V, which correlate with the successive formation of the monocation and dication of **8**. The same holds for the second oxidation of **8** albeit at more positive potentials of +1.19 and +1.26 V. Regarding the reduction, the first reversible reduction of **8** is not split. However, it includes the transfer of two electrons, which, however, coalesce. Gaussian deconvolution affords reductions at −1.03 and −1.12 V. The second reduction exhibits like the first and second oxidations two well-separated reductions at −1.22 and −1.31 V. Once again, sizeable inter-perylene interactions are operative. In general, the same trends were seen for *syn*-isomer **9**. Here, the split for the first and second reduction were unresolvable. Relative to **8**, all reductions are cathodically shifted. Gaussian fittings, which were needed to deconvolute the DPVs, afford reductions at −1.38, −1.59, and −1.62 V. The one-electron oxidations are anodically shifted to +0.64 and +0.74 V as well as to +1.08 V. The larger electrochemical band gap in **9** confirms the hypsochromic shifts seen in the absorption spectra relative to **8**. Interesting is the fact that the inter-perylene couplings are insensitive to the isomeric nature of **8** and **9**.

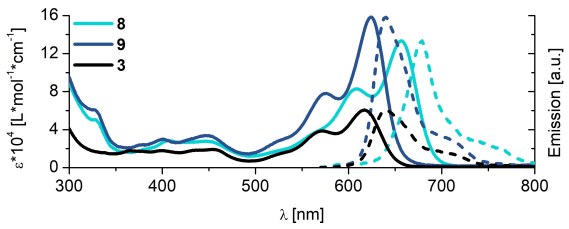

Figure 6. Steady-state absorption (solid lines) and fluorescence spectra (dashed lines) of **8**, **9** and heterodimer **3** in toluene at room temperature.

Table 1. Global fluorescence maxima and corresponding fluorescence quantum yields Φ_{Fl} (in parenthesis) of **8** and **9**.

	Toluene	Anisole	Benzonitrile
8	679 nm (0.13)	683 nm (0.072)	684 nm (0.0083)
9	640 nm (0.47)	648 nm (0.34)	651 nm (0.0080)

Perylene-naphthalene dimers

The synthetic pathway towards homodimeric perylene-perylene chromophores **8** and **9** was not suitable for the synthesis of heterodimeric compounds. A suitable precursor for this purpose is compound **1** (Scheme 1), which was previously developed in our group.[13] A condensation reaction between **1** and naphthalene monoimide (NMI) **10** afforded the perylene-naphthalene chromophores **4** and **5** (Scheme 3). For this purpose, a NMI with sterically demanding swallow tail substituents was synthesized analogously to a literature procedure for perylenes (see Supporting Information).[7]

The crude product was purified *via* several plug chromatographic procedures on silica (CH_2Cl_2:hexanes: 1:1→1:0). Thereby, the two isomers were separated and obtained as a green-turquoise (Rf = 0.6) and a green (Rf = 0.3) solid in 42% and 14%, respectively. Both products were identified *via* high resolution mass spectrometry. In this case, structural elucidation of the isomers is rather complicated due to symmetry reasons. Furthermore, stacking of the molecules leads to a pronounced temperature dependence in the NMR spectra. As a consequence, additional NMR experiments for a detailed assignment of the proton NMR signals were not possible. To confirm our assignment of the aromatic protons (Figure 7), we compared

Table 2. Redox potentials versus Fc/Fc^+ of **8**, **9**, and **3** as obtained from differential pulse voltammetry.

	E_{red}^2	E_{red}^1	E_{ox}^1	E_{ox}^2
8	−1.22/−1.31	−1.03/−1.12	+0.79 / +0.89	+1.19 / +1.26
9	−1.59/−1.62	−1.38	+0.64 / +0.74	+1.08
3	−1.24	−1.06	+0.81	+1.19

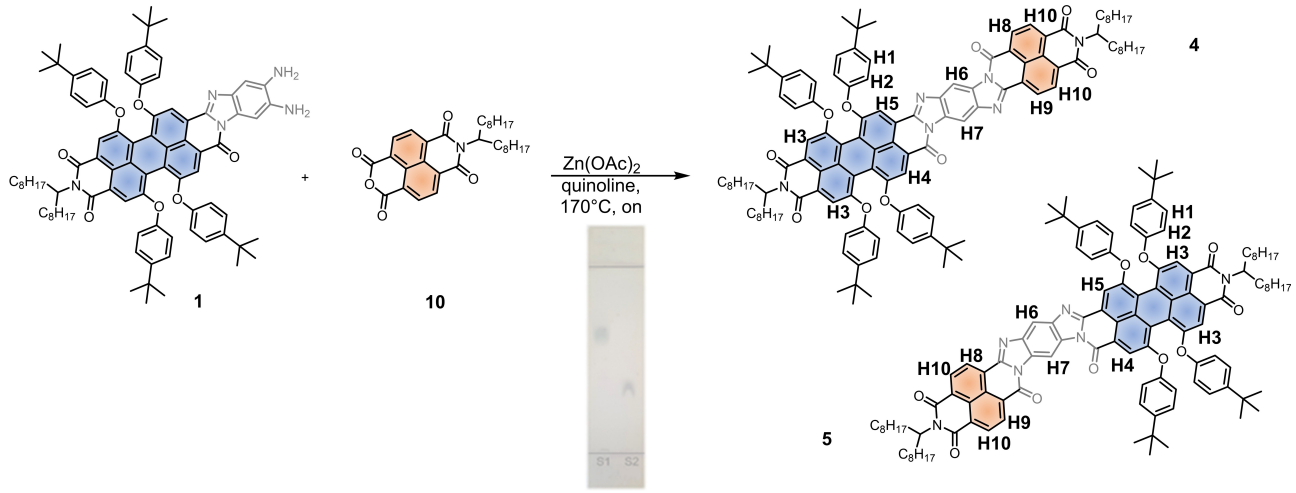

Scheme 3. Condensation of perylene precursor **1** with naphthalene monoimide **10** towards the *anti*- and *syn*-isomers **4** and **5** of perylene-naphthalene heterodimer. Inset: picture of the newly separated sample on a TLC-SiO_2 plate (CH_2Cl_2).

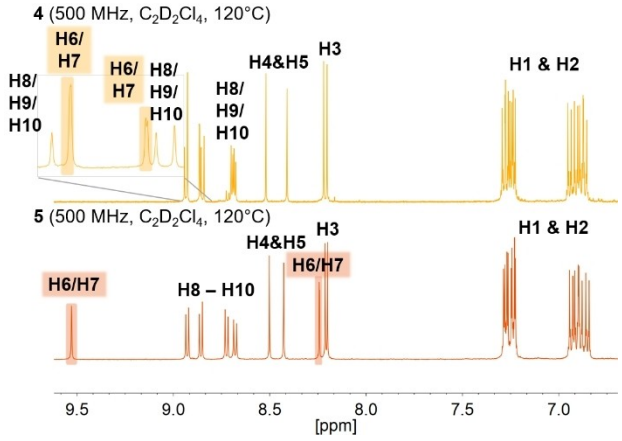

Figure 7. Assumption of signal assignment in perylene-naphthalene dimers **4** and **5**. For the assignment see Scheme 3.

these spectra with those of the similar and fully characterized perylene-perylene dimers **8** and **9**. The characteristic signal groups in the range from 7.29–6.84 ppm belong to the 16 aromatic protons H1 and H2 of the *bay* substituents. Another similarity are the four singlets for the perylene hydrogens H3–H5 that gave the same pattern as found for the homodimeric compounds. Two of the four singlets around 8.20 ppm are not influenced by the different configurations of the bridging unit. Accordingly, they seem to be the outer perylene protons H3. Some signals in the range from 8.93–8.68 ppm show a strong roof-effect with similar coupling constants $J \approx 7.7$ Hz. These four duplets stem from the naphthalene core H8–H10. Moreover, these signals cover two protons H6 and H7 for the bridging unit in one case (upper spectrum, marked in light orange). However, these protons are clearly separated signals at $\delta = 9.53$ and 8.24 ppm for the other isomer. A comparison of the positions of H6 and H7 in both spectra, leads to the assumption, that the light orange spectrum belongs to the *anti*-isomer **4**. The *syn*-configuration of the bridging imide groups is expected to give signals that are further shifted from each other as they are for the *anti*-configuration. Hence, the dark orange spectrum is attributed to the *syn*-isomer **5**.

Steady-state absorption and fluorescence of perylene-naphthalene heterodimers

Perylene-naphthalene heterodimers **4** and **5** feature absorption maxima in the spectral regions from 330 to 500 nm, that is, at 335 and 450 nm, respectively, and in the spectral regions from 500 to 650 nm, that is, at 582 and 629 as well as 566 and 612 nm – Figures 8, S29 and S30. For *anti*-dimer **4** the absorptions are generally red-shifted in comparison to **5** similar to the findings seen for the corresponding perylene-perylene homodimers.

The fluorescence spectra are near-mirror images of the respective absorption spectra with maxima at 657 and 636 nm for **4** and **5**, respectively. Correspondingly, we calculated the HOMO-LUMO gaps as 1.93 (**4**) and 1.99 eV (**5**). Similar to their perylene-perylene homodimers, the fluorescence quantum yields are rather high, but drop significantly as the polarity of the solvent is increased to anisole and benzonitrile – Table 3.

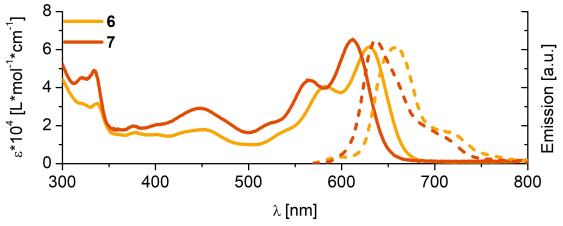

Figure 8. Steady-state absorption (solid lines) and fluorescence spectra (dashed lines) of **4** and **5** in toluene at room temperature.

Table 3. Global fluorescence maxima and corresponding fluorescence quantum yields Φ_{Fl} (in parenthesis) of **4** and **5**.

	Toluene	Anisole	Benzonitrile
4	657 nm (0.27)	663 nm (0.043)	665 nm (0.016)
5	636 nm (0.43)	646 nm (0.039)	650 nm (0.0070)

Electrochemistry of perylene-naphthalene heterodimers

When turning to the oxidation of **4** (Table 4 and Figures S31–33), four one-electron processes are identified at +0.75, +0.84, +1.04, and +1.11 V. Here, the first and fourth oxidations are perylene-centered, while the second and third oxidations are centered on naphthalene. For **5**, all oxidations are anodically shifted relative to **4**. The only exception is the fourth oxidation, which is outside of the accessible window. On the reductive side, four one-electron reductions are noted at −1.08, −1.21, −1.36, and −1.58 V. Once again, the first and second of them are assigned to be perylene-centered, while the third and fourth process relate to naphthalene-centered reductions. Importantly, the first reversible one-electron reduction of naphthalene in **4** is cathodically shifted relative to a reference.[17] From the latter we conclude an appreciable electronic coupling between perylene and naphthalene. For **5**, all reductions are subject to subtle anodic shifts. Similar to the findings with the homodimers **8** and **9**, where the reduction/oxidation of one perylene affects that of the other, the reduction/oxidation of the perylene impacts the reduction/oxidation of the naphthalene in the heterodimers **4** and **5**.[18]

Table 4. Redox potentials versus Fc/Fc^+ of **4** and **5** as obtained from differential pulse voltammetry: pery and naph indicate perylene- and naphthalene-centered reductions/oxidations, respectively.

	E_{red}^2		E_{red}^1			E_{ox}^1		E_{ox}^2
	naph	naph	pery	pery	pery	naph	naph	pery
4	−1.58	−1.36	−1.21	−1.08	+0.75	+0.84	+1.04	+1.11
5	−1.51	−1.31	−1.15	−1.05	+0.81	+0.92		+1.15

Modifications of the bridging unit

Both aforementioned examples demonstrate facile pathways towards perylenes with linearly elongated aromatic systems. The associated bathochromic shifts in the absorption spectra could be enhanced upon the addition of trifluoroacetic acid (TFA) to solutions of the regioisomerically pure perylene-perylene and perylene-naphthalene dimers in chloroform (Figure 9). However, the peaks are broadened and the typical signal splitting for perylene compounds is lost after protonation. The color differences of the neutral species converge to purple in the case of **8** and **9** and lush green for **4** and **5**.

In previous examples we attributed these shifts to a protonation of the unsubstituted N-atoms at the bridging unit. A theoretical bathochromic shift of 92 nm between the neutral and the two-fold protonated species of *anti*-perylene-perylene was obtained by quantum mechanical calculations.[11] This outcome fits perfectly with our experimentally determined shift for the *anti*-isomer. Table 5 sums up the results for the protonation experiments with the four isomers.

Whereas the neutral species of **8** and **9** differ significantly in their absorption (31 nm), they reveal similar maxima after the addition of TFA. The situation is very similar for the perylene-naphthalene isomers **4** and **5**. The color changes are reversible by the addition of a weak organic base such as pyridine or by evaporation of the acid (see Supporting Information).

We also performed titration experiments with the chromophores and TFA in chloroform (Figure 10). The arrows are indicating the decreasing and increasing extinction coefficients of the main absorption bands. The continuous red-shift occurs faster at low acid concentrations and saturates at higher concentrations (see Supporting Information). No isosbestic points were observed for the measurements.

The fluorescence emission bands (Figure 11) are red-shifted as well with increasing amounts of TFA. Overall, a quenching to lower emission intensities is obtained. In the case of **4**, the emission rises towards a maximum value at $\lambda = 724$ nm, before it starts to decrease. For the isomers **8**, **9**, and **5** a novel emission band arises after the main absorption band has

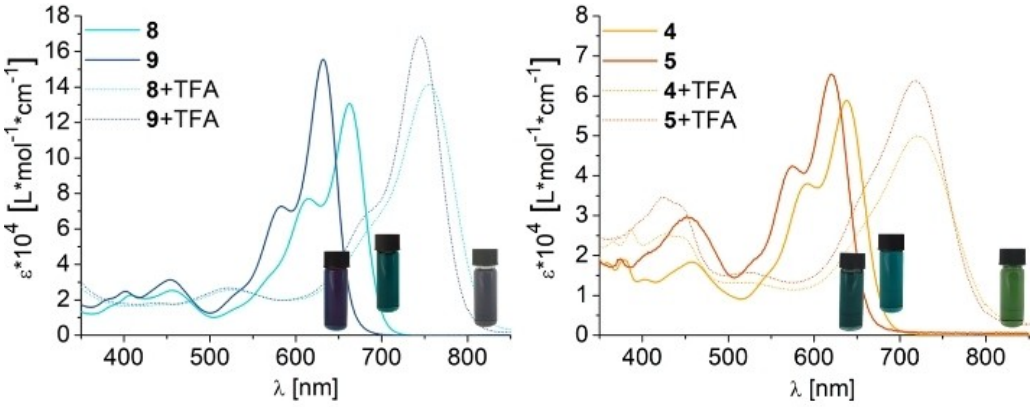

Figure 9. Absorption spectra of perylene-perylene (left) and perylene-naphthalene (right) isomers in chloroform and TFA.

Table 5. Maxima of the main absorption bands of the neutral and protonated forms of perylene-perylene and perylene-naphthalene isomers measured in chloroform at room temperature.

Neutral species	λ_{max} abs. [nm]	TFA [% v/v][a]	Protonated species	λ_{max} abs. [nm]
8	663	70	**1**	755
9	632	50	**2**	745
4	638	90	**6**	720
5	620	70	**7**	717

[a] amount of TFA where the maximum red-shift could be obtained.

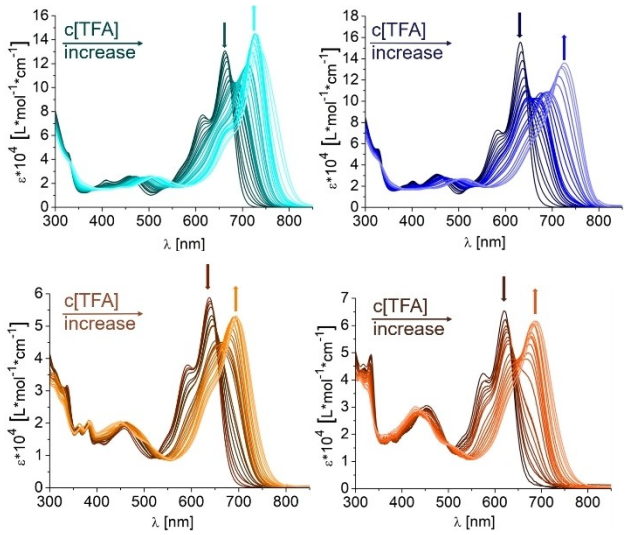

Figure 10. UV/Vis titrations of **8** (top left), **9** (top right), **4** (bottom, left), and **5** (bottom, right) with TFA in chloroform.

disappeared. Though, at high TFA concentrations, only very weak emission bands are found.

Changes in terms of redox potentials of the perylenes units in the homodimers and heterodimers as a function of bridge protonation were also studied (Table 6). DPVs were recorded in the presence of TFA, at concentrations which mainly accounted for the mono-protonation at the nitrogen atoms in the bridge. Clear evidence was found for the elimination of the coupling between the two perylenes in homodimers **8** and **9** (Figures S38-S41). In particular, the overlapping/coupled first oxidation disintegrated into two separate one-electron oxidations at +0.84 and 1.01 V, for **8**. In **9**, these oxidations were observed at +0.85 and +1.04 V. We rationalize our observation that mono-protonation of the bridge creates two different, inequivalent environments for the two perylenes. This, in turn, causes the first oxidation associated with each perylene to occur at two separate potentials. A similar behaviour evolves for the second oxidation and the reduction. In line with the substantial red-shifts in the absorption assays, the reductions of homodimers **8** and **9** is subject to a 0.4 V shift towards less negative values. The aforementioned is well in line with overall smaller HOMO-LUMO gaps.

When turning to mono-protonated heterodimers **4** and **5** similar trends to those described for homodimers **8** and **9** in terms of anodic shifts of the reductions were concluded (Figures S42-S45). The reductions associated with perylene and naphthalene both shift to less negative values by ~0.86 V. Only two one-electron oxidations were, however, observed. For **4**, these are located at +0.91 and +1.1 V. Owing to the fact that protonation cancels the coupling between naphthalene and perylene, oxidations of the earlier are likely to shift to positive potentials outside of the experimental range. As such, only oxidations, which are associated with perylene, are noted. This leads to a similar gap between the first and second oxidation of

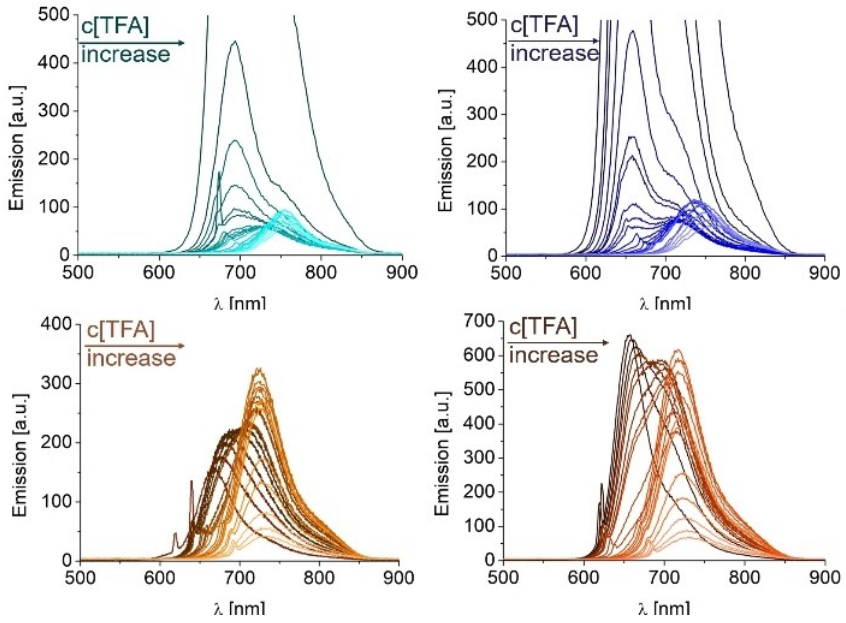

Figure 11. Fluorescence titrations of **8** (top left), **9** (top right), **4** (bottom, left), and **5** (bottom, right) with TFA in chloroform (excitations at λ_{max} abs).

Table 6. Redox potentials versus Fc/Fc^+ of perylene-perylene and perylene-naphthalene isomers in the presence of TFA accounting for mono-protonation as obtained from differential pulse voltammetry.

	E_{red}^2		E_{red}^1		E_{ox}^1		E_{ox}^2
8+TFA	−0.88		−0.61		+0.84	+1.01	+1.28
9+TFA	−0.79		−0.55		+0.85	+1.04	+1.29
	E_{red}^4	E_{red}^3	E_{red}^2	E_{red}^1		E_{ox}^1	E_{ox}^2
4+TFA	−0.73	−0.53	−0.41	−0.27	−0.21	+0.91 +1.10	+1.34
5+TFA	−0.62	−0.44	−0.34	−0.22	−0.15	+098 +1.18	+1.43

0.2 V as seen for homodimers **8** and **9**. This suggests that the two oxidations relate to the first oxidation of the two perylenes, which are in different environments. Notable, we assume an equal probability for the nitrogen protonation in either close proximity to naphthalene or to perylene. The same trend emerged for the first reduction of **4** (−0.21/−0.27 V) and **5** (−0.15/−0.22 V) upon protonation. In particular, two closely spaced reductions, which presumably involve the two perylenes in different environments, evolve as a result of protonation of either perylene or naphthalene. In general, for **5**, reductions are subject to subtle anodic shifts.

Since the protonated forms of linearly elongated perylenes showed such interesting optical characteristics, we wanted to reproduce the outcome without the use of TFA. The addition of acid hinders the utilization of the chromophores for many applications. Hence, we modified the bridging units with methyl groups. As an example, for one-fold methylated perylene dimers, previously reported perylene-phenanthrene **11**[13] was reacted with methyl iodide (Scheme 4). Therefore, **11** was stirred in an excess of methylation reagent for several days at room temperature. After the starting material has disappeared, methyl iodide was evaporated and Ag(OTf) in a CH_2Cl_2/ACN mixture was added to obtain the stable triflate as counter-ion. Extraction in CH_2Cl_2 led to the dark green mono-methylated product without further purification.

As expected, the methylation took place only at the anhydride-amine fused side. The product was identified *via* high-resolution mass spectrometry (MALDI-TOF MS, dctb) with an error of 1.8. The success of the reaction could be further proven *via* proton NMR spectroscopy. Figure 12 shows the characteristic signals for the unmethylated and one-fold methylated perylene-phenanthrene dimers **11** and **12** (see Scheme 4 for assignment). A new singlet at 3.98 ppm (marked in pink) emerged after methylation that represents the novel methyl group H12 at the N-atom of the bridging unit. It was identified *via* the lack of a cross-peak in COSY spectrum. Other characteristic signals are two multiplets in the range from 7.41–6.93 ppm for the aromatic protons H1 and H2 of the *bay* substituents. These signals and the signal groups for phenanthrene protons H8–H11 were identified *via* a COSY measurement. A correlation between H6 and H7 in HMBC spectrum identified these signals as bridge protons. However, only H6 shows a cross-peak with the methyl group and is therefore attributed to the singlet at 9.13 ppm. Consequently, the signal at 8.40 ppm is identified as H7. Whereas the outer perylene protons H3 reveal quite similar shifts (8.32 and 8.31 ppm), the signals for H4 and H5, near the phenylene bridge, are rather different. Proton H5, which shows a cross-peak with the methyl group, belongs to the singlet at 8.07 ppm. The more downfield shifted signal at $\delta = 8.30$ ppm represents perylene-proton H4.

The color change of the perylene-phenanthrene dimer from dark blue towards dark green after methylation is shown in Figure 13. As a result, a pronounced red-shift of its main absorption band from 621 nm[13] towards 692 nm takes place. Nonetheless, the methylated chromophore shows a less pronounced fine-structure and reveals a slightly lower extinction coefficient. The fluorescence maximum is red-shifted by 88 nm.

As a matter of fact, mono-methylation of the bridging unit had a significant effect on the optical features of the linearly elongated perylene-phenanthrene dimer. For further investigation of the methyl group assisted protonation and its influence on the absorption and emission properties, bis-methylated species were synthesized. For this purpose, we reacted the *anti*- and *syn*-isomers **8** and **9** of perylene-perylene dimer with methyl iodide. After one week there was still some starting material left in the reaction mixture. Therefore, we decided to use a stronger methylation reagent. The utilization of methyl triflate eventually led to the bis-methylated triflates **13** and **14**

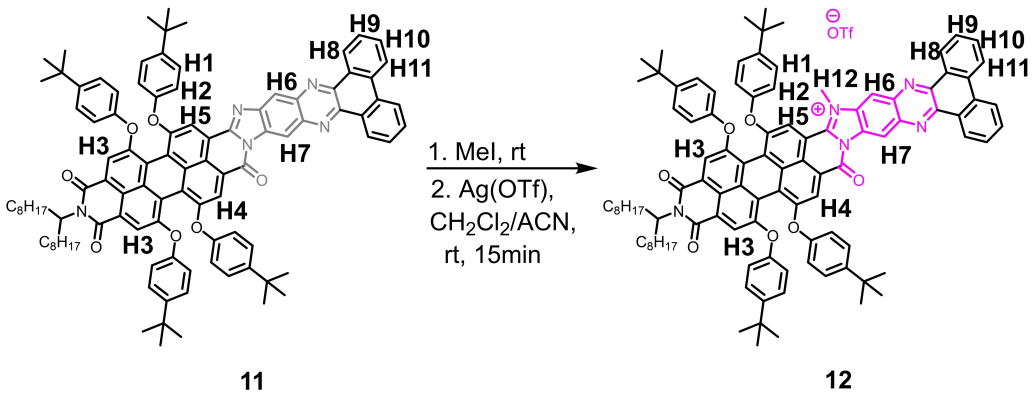

11 12

Scheme 4. Methylation of perylene-phenanthrene **11** *via* methyl iodide.

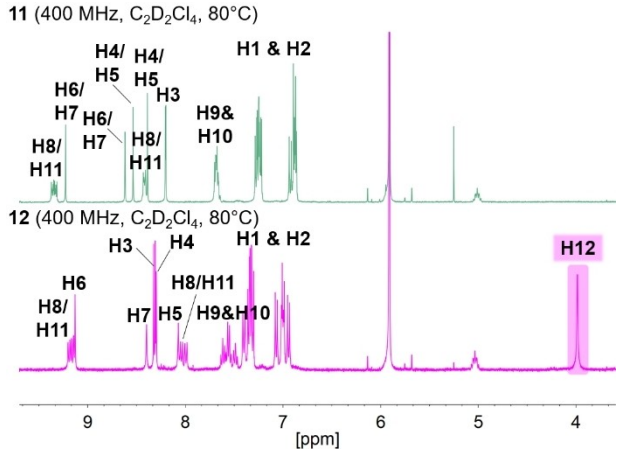

Figure 12. Characteristic signals of neutral and methylated perylene-phenanthrene dimers **11** and **12**. For the assignment see Scheme 4.

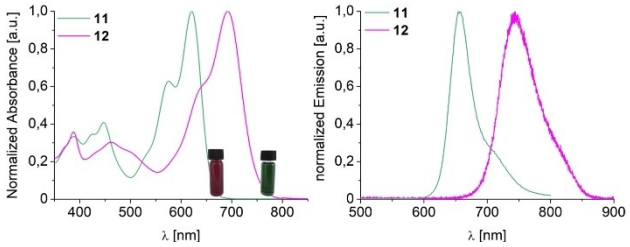

Figure 13. UV/Vis (left) and fluorescence (right) spectra of unmethylated and methylated perylene-phenanthrene dimer **11** and **12** in chloroform.

(Figure 14). Their isolation didn't require further purification. Surprisingly, high-resolution mass spectrometry provided only a signal of the monomethylated species, whereas no signals for the expected bis-methylated species were obtained. Most likely, the isotopic pattern of the signal attributed to $C_{170}H_{191}N_6O_{15}$ arises from triflate replacement by a water molecule in the mass spectrometer, followed by a loss of one proton. Such transformations of higher charged complexes have been reported before.[19] However, ^{19}F NMR spectrometry showed a strong signal for the free triflate counter ion for **13** at −78.07 ppm and for **14** at 78.02 ppm. (see Supporting Information).

Further NMR measurements were performed to fully characterize the structure of the methylated chromophores. Figure 15 shows important parts of both proton NMR spectra. All signals in the aromatic regions of **13** and **14** are shifted downfield compared to the unmethylated species. However, the signal splitting stayed the same after methylation. The main differences are the singlets H7 at 4.16 ppm and H8 at 4.32 ppm (marked in purple) for the methyl groups. These signals not only confirm a successful reaction, but also contribute to a detailed assignment of the aromatic protons. Especially the inner perylene-protons H4 and the hydrogens H6 at the benz-bisimidazole bridges are influenced by these groups and show correlations with the latter in the HMBC spectra (see Supporting

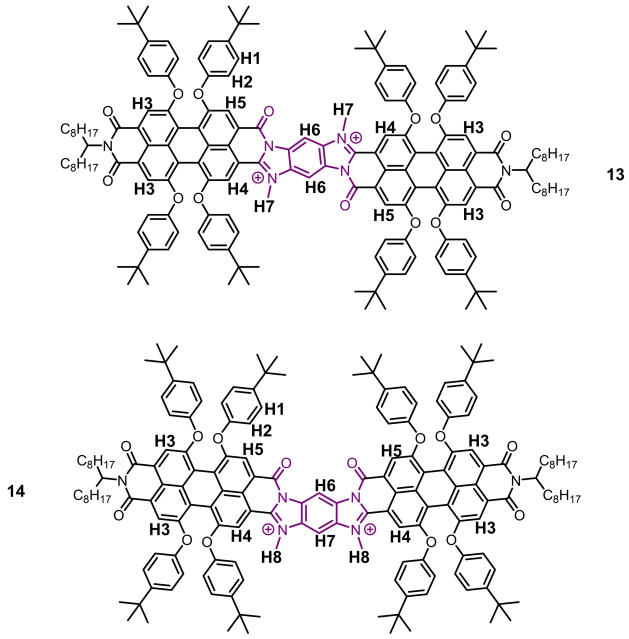

Figure 14. Two-fold methylated *anti*- **13** and *syn*- **14** perylene-perylene dimers.

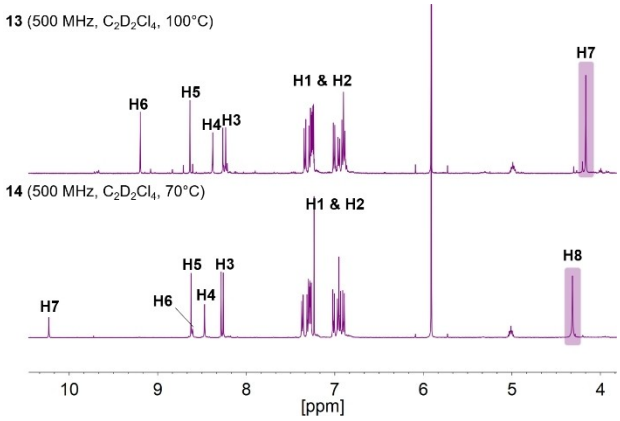

Figure 15. Interesting regions of ^1H NMR spectra of the methylated chromophores **13** and **14**. For the assignment of signals see Figure 14.

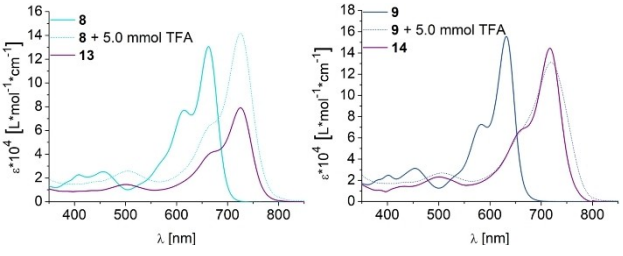

Figure 16. Absorption spectra of the neutral, protonated and methylated species of *anti*- (left) and *syn*- (right) configurated perylene-perylene-dimers.

Information). Thereby, the singlets at 8.38 ppm for **13** and 8.47 ppm for **14** could be identified as H4 and the signals at

9.20 ppm for **13** and 8.61 ppm for **14** can be assigned to H6. The remaining hydrogens of the perylene scaffold, H3 and H5, show similar shifts for both isomers. Due to symmetry reasons, the dimer with *syn*-configuration has a second bridge proton H7 that is strongly influenced by two carbonyl groups and is shifted downfield to 10.23 ppm.

The absorption spectra of the methylated dimers are displayed in Figure 16. To ease the comparisons, the graphs of the unmethylated and the protonated species are added. As expected, a pronounced red-shift is observed upon methylation of the perylene-perylene chromophores. Modified *anti*-isomer **13** is shifted by 62 nm, whereas *syn*-isomer **14** reveals a stronger bathochromic shift of 87 nm compared to the unmethylated species. Thereby, the absorption maxima became similar for both isomers **13** (λ_{max} = 725 nm) and **14** (λ_{max} = 719 nm). However, both methylated species could not reach the extraordinary far red-shift that was obtained by protonations with TFA. The absorption maxima of the dimers with 5.0 mmol TFA fit the maxima of the twofold methylated species. Thus, it seems as if other positions in the molecules were protonated after the addition of more than 5.0 mmol TFA.

The fluorescence maxima are red-shifted by 64 nm for the *anti*- and 96 nm for the *syn*-isomers (see Supporting Information). Consequently, bis-methylation of the dibenzimidazole-bridging-unit of both perylene-perylene regioisomers leads to a weakening of the structural *anti*-/*syn*-effect. Therefore, only small differences between the optical properties of the isomers are obtained. This outcome is in contrast to the unmethylated species, where the absorption and emission maxima of *anti*-isomer **8** are notably red-shifted compared to those of its *syn*-analogue **9**.

Conclusions

We have developed efficient synthesis and purification strategies to access regioisomerically pure *syn*- and *anti*-isomers of linearly elongated rylene chromophores with 30 and 35 conjugated π-electron pairs. The absorption and fluorescence properties of the perylene-perylene and the perylene-naphthalene isomers are solvent dependent, and all chromophores have given rise to high fluorescence-quantum yields as well as two oxidations and two reductions. As expected, the smaller perylene-naphthalenes absorb at shorter wavelengths, than their perylene-perylene counterparts. Furthermore, we succeeded in further narrowing the HOMO-LUMO gaps of the isomers *via* protonation and methylation of the dibenzimidazole-bridging-units of the perylene-perylene dimers. Upon these modifications, the absorption and emission maxima became similar for the *anti*- and *syn*-isomers. Compared to the variation of the π-system length, the modifications at the bridging units have a more pronounced effect on the optical properties of the chromophores. Further investigations on the influence of the bridging units are underway in our laboratories.

Experimental Section

General: Chemicals were ordered from SIGMA ALDRICH, ACROS ORGANICS or ALFA AESAR and were used as received. Quinoline was freshly distilled and handled under nitrogen atmosphere. All experiments were performed at room temperature and under atmospheric conditions with magnetic stirring unless stated otherwise. Plug chromatographies were performed on a filter funnel (P3, length: 17 cm, diameter: 5.2 cm) Proton nuclear magnetic resonance (^{1}H NMR) and carbon nuclear magnetic resonance (^{13}C NMR) spectra were recorded on a Bruker Avance Neo spectrometer (400 MHz and 500 MHz for ^{1}H NMR, 101 MHz and 126 MHz for ^{13}C NMR). The samples were dissolved in deuterated solvents, chemical shifts are given in ppm and were referenced to the solvent residual peak (^{1}H: δ = 5.32 ppm, ^{13}C: δ = 53.8 ppm for CH_2Cl_2 and ^{1}H: δ = 5.91 ppm, ^{13}C: δ = 74.2 ppm for $C_2D_2Cl_4$). Mass spectrometry was carried out with a UltrafleXtreme instrument (MALDI-TOF, matrix: 2,5-dihydroxybenzoic acid DHB, trans-2-[3-(4-tert-butylphenyl)-2-methyl-2propenyliden] malononitrile, DCTB) or without matrix (OM). A Perkin Elmer Lambda 2 instrument was used for UV/Vis spectroscopy measurements measured against the solvent. The fluorescence spectra were obtained with a Horiba Fluoromax 3. The electrochemistry data was recorded using a three-electrode system with $[NBu_4][PF_6]$ as the electrolyte in a home-made cell. The glassy carbon, Pt wire and Ag wire were used as the working, counter and reference electrode, respectively. Fc/Fc^+ was employed as the internal reference, in order to correct the redox potentials of the molecules.

Perylene-perylene dimers 8 and 9: In a dry flask degassed quinoline (5 mL) and 1,2,4,5-benzenetetramine **9** (9.83 mg, 71.2 μmol, 1 eq.) were suspended. Triethylamine (59.5 μL, 0.427 mmol, 6 eq.) was added dropwise and the solution was stirred for 30 minutes. After the triethylamine was vaporized by a vacuum pump perylenemonoimide **6** (200 mg, 0.164 mmol, 2.3 eq.) and dry $Zn(OAc)_2$ (45.7 mg, 0.249 mmol, 3.5 eq.) were added to the solution and stirred at 160 °C for 44 h. The solvent was evaporated, and the crude product was purified by plug chromatographies (silica, CH_2Cl_2:hexanes 3:7→1:1) to get the *anti*- (41.9 mg, 16.7 μmol, 23%) and the *syn*-(58.2 mg, 23.2 μmol, 33%) isomer.

Anti-isomer **8**: ^{1}H NMR (500 MHz, $C_2D_2Cl_4$, 100 °C): δ [ppm] = 8.83 (s, 2H), 8.47 (s, 2H), 8.41 (s, 2H), 8.20 (s, 2H), 8.19 (s, 2H), 7.27–7.20 (m, 16H), 6.91–6.85 (m, 16H), 5.04–4.98 (m, 2H), 2.11–2.06 (m, 4H), 1.84–1.77 (m, 4H), 1.30 (d, J = 2.2 Hz, 36H), 1.28 (d, J = 1.3 Hz, 36H), 1.25–1.19 (m, 48H), 0.82–0.79 (pseudo-t, 12H); ^{13}C NMR (126 MHz, $C_2D_2Cl_4$, 100 °C): δ [ppm] = 163.9, 159.9, 156.4, 156.4, 156.1, 155.9, 153.6, 153.4, 153.3, 150.1, 147.8, 147.7, 147.7, 147.6, 143.4, 133.9, 132.5, 131.3, 126.9, 126.8, 123.4, 122.3, 121.2, 121.0, 120.7, 120.5, 120.0, 119.5, 119.4, 119.3, 116.7, 107.0, 99.9, 55.2, 34.5, 34.5, 34.5, 32.8, 32.0, 31.7, 31.7, 31.7, 29.7, 29.6, 29.3, 27.3, 22.7, 14.1; HRMS (ESI): m/z calculated for $C_{168}H_{185}N_6O_{14}$: 2510.3943 $[M+H^+]$ found 2510.3875 m/z (error: 2.7).

Syn-isomer **9**: ^{1}H NMR (500 MHz, $C_2D_2Cl_4$, 100 °C): δ [ppm] = 9.52 (d, J = 0.8 Hz, 1H), 8.49 (s, 2H), 8.40 (s, 2H), 8.20 (s, 2H), 8.19 (s, 2H), 8.13 (d, J = 0.8 Hz, 1H), 7.26–7.20 (m, 16H), 6.91–6.82 (m,16H), 5.04–4.98 (m, 2H), 2.10–2.04 (m, 4H), 1.84–1.78 (m, 4H), 1.30 (d, J = 2.4 Hz), 1.28 (d, J = 0.7 Hz, 36H), 1.28–1.19 (m, 48H), 0.82–0.79 (pseudo-t, 12H); ^{13}C NMR (126 MHz, $C_2D_2Cl_4$, 100 °C): δ [ppm] = 164.1, 159.7, 156.3, 156.3, 156.1, 156.0, 153.8, 153.4, 153.3, 153.3, 150.1, 147.9, 147.7, 147.6, 147.5, 143.4, 133.9, 132.53, 130.9, 126.8, 126.8, 126.8, 126.8, 123.3, 122.1, 121.2, 120.9, 120.6, 120.5, 120.0, 119.8, 119.6, 119.5, 119.5, 119.3, 119.3, 117.1, 110.9, 103.2, 99.9, 55.2, 34.5, 34.5, 32.8, 32.0, 31.8, 31.7, 31.7, 31.7, 29.7, 29.59, 29.3, 27.3, 22.7, 14.1; HRMS (APPI): m/z calculated for $C_{168}H_{185}N_6O_{14}$: 2510.3943 $[M+H^+]$ found 2510.3961 m/z (error: −0.7).

Perylene-naphthalene dimers 4 and 5: Chromophore **1** (30.0 mg, 22.7 μmol, 1 eq.), naphthalenemonoimide **10** (11.5 mg, 22.7 μmol, 1 eq.), $Zn(OAc)_2$ (16.0 mg, 87.2 μmol, 3.8 eq.) and degassed quinoline (3.5 mL) were added to a dry flask under nitrogen atmosphere. The solution was stirred overnight at 170 °C. The solvent was evaporated, and the crude product was purified *via* several plug chromatographies (silica, CH_2Cl_2:hexanes: 1:1→1:0). The two isomers were obtained as a green-turquoise (17.0 mg, 9.48 μmol, 42%, *anti*- isomer) and a green (5.9 mg, 3.29 μmol, 14%, *syn*-isomer) solid.

Anti-isomer **4**: ^{1}H NMR (500 MHz, $C_2D_2Cl_4$, 120 °C): δ [ppm] = 8.93 (d, J = 7.8 Hz, 1H), 8.93 (s, 1H), 8.86 (d, J = 0.8 Hz, 1H), 8.85 (d, J = 7.6 Hz, 1H), 8.69 (d, J = 7.7 Hz, 1H), 8.68 (d, J = 7.6 Hz, 1H), 8.52 (s, 1H), 8.41 (s, 1H), 8.22 (s, 1H), 8.20 (s, 1H), 7.29-.23 (m, 8H), 6.95–6.85 (m, 8H), 5.12–5.06 (m, 1H), 5.06–5.00 (m, 1H), 2.17–2.08 (m, 4H), 1.90–1.81 (m, 4H), 1.34 (s, 9H), 1.33 (s, 9H), 1.31 (s, 9H), 1.30 (s, 9H), 1.29–1.21 (m, 48 H), 0.84–0.81 (pseudo-t, 12H); HRMS (MALDI-TOF, dctb): m/z calculated for $C_{118}H_{132}N_6O_{10}$: 1793.0005; m/z found: 1792.9999 [M + $^+$] (error: 1.2).

Syn-Isomer **5**: ^{1}H NMR (500 MHz, $C_2D_2Cl_4$, 110 °C): δ [ppm] = 9.53 (s, 1H), 8.93 (d, J = 7.7 Hz, 1H), 8.86 (d, J = 7.6 Hz, 1H), 8.72 (d, J = 7.6 Hz, 1H), 8.68 (d, 1H, J = 7.7 Hz), 8.50 (s, 1H), 8.43 (s, 1H), 8.24 (d, J = 0.7 Hz, 1H), 8.21 (s, 1H), 8.20 (s, 1H), 7.29–7.26 (m, 4H), 7.25–7.22 (m, 4H), 6.94–6.84 (m, 8H), 5.12–5.06 (m, 1H), 5.05–5.00 (m, 1H), 2.19–2.06 (m, 4H), 1.90–1.79 (m, 4H), 1.33 (s, 9H), 1.33 (s, 9H), 1.33 (d, 0.7 Hz, 18H), 1.26–1.21 (m, 48H), 0.83–0.81 (pseudo-t, 12H); HRMS (APPI): m/z calculated for $C_{118}H_{133}N_6O_{10}$: 1794.0078; m/z found: 1794.0110 [M + H^+] (error: −1.8).

1-Fold methylated Per-phenanthrene 12: In a dry vial 9 mg of Perylene-Phenanthrene (6.0 μmol) and 2 mL methyliodide (32 mmol) were added and stirred for several days at room temperature. After all educt was consumed (TLC), methyliodide was evaporated and Ag(OTf) (3 mg, 12 μmol) in CH_2Cl_2/ACN (1:1, 6 mL) was added and stirred for 15 min. The volatiles were removed and the crude product was extraced in CH_2Cl_2 to yield 5.5 mg of the methylated product. ^{1}H NMR (400 MHz, $C_2D_2Cl_4$, 80 °C): δ [ppm] = 9.20–9.14 (m, 2H), 9.13 (s, 1H), 8.40 (s, 1H), 8.32 (s, 1H), 8.31 (s, 1H), 8.30 (s, 1H), 8.07 (s, 1H), 8.04 (d, J = 8.1 Hz, 1H), 7.99 (d, J = 8.1 Hz, 1H), 7.64–7.47 (m, 4H), 7.41–7.30 (m, 8H), 7.08–6.93 (m, 8H), 5.07–5.00 (m, 1H), 3.98 (s, 3H), 2.13–2.05 (m, 2H), 1.88–1.80 (m, 2H), 1.35 (d, J = 2.1 Hz, 9H), 1.32 (d, J = 1.6 Hz, 9H), 1.27–1.20 (m, 24H), 0.83–0.80 (pseudo-t, 6H); ^{13}C NMR (101 MHz, $C_2D_2Cl_4$, 80 °C): δ [ppm] = 163.8, 158.9, 158.6, 157.5, 156.5, 155.8, 152.7, 152.6, 152.4, 149.5, 149.3, 148.9, 148.8, 148.7, 148.5, 148.3, 143.5, 143.2, 140.3, 140.0, 134.4, 133.3, 132.4, 132.3, 131.8, 131.7, 131.5, 129.5, 129.3, 128.8, 128.6, 128.1, 127.5, 127.3, 127.3, 127.2, 126.9, 126.8, 126.2, 124.7, 123.0, 122.9, 122.0, 120.5, 120.2, 119.8, 119.8, 119.44, 119.0, 118.5, 117.1, 111.4, 110.6, 55.6, 35.7, 35.7, 34.8, 34.7, 34.7, 32.8, 32.0, 31.7, 31.7, 31.7, 31.7, 29.7, 29.6, 29.4, 27.3, 22.8, 14.2. (MALDI-TOF, dctb): m/z calculated for $C_{102}H_{104}N_5O_7$: 1510.7930; m/z found: 2510.7903 [M + $^+$] (error: 1.8).

2-Fold methylated *anti*-Per–Per 13: *Anti*-isomer **8** of Per-Per (11 mg, 4.4 μmol), MeOTf (50 μL, 0.46 mmol), the tip of a spatula of K_2CO_3 and anhydrous $CHCl_3$ (1.0 mL) were added to a dry vial under nitrogen atmosphere. The reaction was stirred several days at room temperature. The volatiles were removed, CH_2Cl_2 was added and the mixture was filtered to yield 10 mg of the two-fold methylated product. ^{1}H NMR (500 MHz, $C_2D_2Cl_4$, 70 °C): δ [ppm] = 9.20 (s, 2H), 8.64 (s, 2H), 8.38 (s, 2H), 8.26–8.23 (m, 4H), 7.34–7.24 (m, 16H), 7.02–6.89 (m, 16H), 5.02–4.96 (m, 2H),4.16 (s, 1H), 2.08–2.02 (m, 4H), 1.82–1.76 (m, 4H), 1.29 (s, 36H), 1.28 (d, 2.0 Hz, 36H), 1.22–1.17 (m, 24H), 0.80–0.77 (pseudo-t, 12H). ^{13}C NMR (126 MHz, $C_2D_2Cl_4$, 70 °C): δ [ppm] = 158.8, 158.7, 158.6, 156.7, 156.2, 152.7, 152.6, 152.5, 152.5, 149.4, 148.6, 148.6, 148.5, 147.9, 134.1, 133.6, 131.3, 128.3, 127.4, 127.3, 127.2, 127.1, 125.8, 125.4, 122.6, 120.6, 120.4, 120.1, 119.9, 119.8, 119.8, 119.4, 119.4, 119.2, 118.9, 118.6, 111.0, 102.1, 55.5, 35.9, 34.2, 32.7, 32.0, 31.7, 31.7, 31.7, 29.9, 29.7, 29.6, 29.4, 27.3, 22.9, 22.8, 14.3, 14.3; HRMS (MALDI-TOF, dctb): m/z calculated for $C_{170}H_{191}N_6O_{15}$: 2556.4362; m/z found: 2556.4352 [M + $^+$] (error: 0.4).

2-Fold methylated *syn*-Per–Per 14: *Syn*-isomer **9** of Per-Per (10 mg, 4.0 μmol), MeOTf (50 μL, 0.46 mmol), the tip of a spatula of K_2CO_3 and anhydrous $CHCl_3$ (1.0 mL) were added to a dry vial under nitrogen atmosphere. The reaction was stirred several days at room temperature. The volatiles were removed, CH_2Cl_2 was added and the mixture was filtered to yield 11 mg of the two-fold methylated product. ^{1}H NMR (500 MHz, $C_2D_2Cl_4$, 100 °C): δ [ppm] = 10.23 (s, 1H), 8.62 (s, 2H), 8.61 (s, 1H), 8.47 (s, 2H), 8.28 (s, 2H), 8.26 (s, 2H), 7.37–7.26 (m, 16H), 7.03–6.89 (m, 16H), 5.03–4.99 (m, 2H), 4.32 (s, 6H), 2.11–2.04 (m, 4H), 1.85–1.78 (m, 4H), 1.32 (s, 18H), 1.31 (s, 18H), 1.30 (s, 36 H), 1.28–1.18 (m, 48H), 0.82–0.79 (pseudo-t, 12H); ^{13}C NMR (126 MHz, $C_2D_2Cl_4$, 100 °C): δ [ppm] = 163.6, 158.9, 158.7, 157.9, 156.8, 156.2, 152.7, 152.7, 152.5, 149.7, 148.8, 148.8, 148.6, 147.8, 134.3, 133.6, 131.4, 128.0, 127.5, 127.2, 127.2, 127.1, 125.9, 125.3, 122.6, 120.6, 120.2, 119.8, 119.8, 119.7, 119.4, 119.3, 118.9, 118.5, 118.0, 110.9, 106.6, 99.7, 55.6, 36.5, 34.7, 34.6, 34.6, 34.6, 32.8, 31.9, 31.7, 31.7, 31.6, 29.7, 29.6, 29.3, 27.2, 22.7, 14.1; HRMS (MALDI-TOF, dctb): m/z calculated for $C_{170}H_{191}N_6O_{15}$: 2556.4362; m/z found: 2556.4352 [M + $^+$] (error: 0.4).

Acknowledgements

The authors thank the Deutsche Forschungsgemeinschaft (DFG – SFB 953 „Synthetic Carbon Allotropes“) for financial support. Open access funding enabled and organized by Projekt DEAL.

Conflict of Interest

The authors declare no conflict of interest.

Keywords: Chromophores · Dyes/Pigments · Methylation · Perylene · π Conjugation

[1] a) T. Weil, T. Vosch, J. Hofkens, K. Peneva, K. Müllen, *Angew. Chem. Int. Ed.* **2010**, *49*, 9068; *Angew. Chem.* **2010**, *122*, 9252–9278; b) F. Würthner, *Chem. Commun.* **2004**, 1564; c) T. Weil, T. Vosch, J. Hofkens, K. Peneva, K. Müllen, *Angew. Chem. Int. Ed.* **2010**, *49*, 9068–9093; *Angew. Chem.* **2010**, *122*, 9252.
[2] a) M. A. Kobaisi, S. V. Bhosale, K. Latham, A. M. Raynor, S. V. Bhosale, *Chem. Rev.* **2016**, *116*, 11685; b) F. Würthner, S. Ahmed, C. Thalacker, T. Debaerdemaeker, *Chem. Eur. J.* **2002**, *8*, 4742; c) X. Guo, M. D. Watson, *Org. Lett.* **2008**, *10*, 5333.
[3] a) C. Huang, S. Barlow, S. R. Marder, *J. Org. Chem.* **2011**, *76*, 2386; b) A. Herrmann, K. Müllen, *Chem. Lett.* **2006**, *35*, 978; c) A. Nowak-Król, F. Würthner, *Org. Chem. Front.* **2019**, *6*, 1272.
[4] Z. Yuan, S.-L. Lee, L. Chen, C. Li, K. S. Mali, S. de Feyter, K. Müllen, *Chem. Eur. J.* **2013**, *19*, 11842.
[5] G. Seybold, *Dyes Pigm.* **1989**, *11*, 303.
[6] a) A. C. Grimsdale, K. Müllen, *Angew. Chem. Int. Ed.* **2005**, *44*, 5592; *Angew. Chem.* **2005**, *117*, 5732–5772; b) H. Langhals, *Helv. Chim. Acta* **2005**, *88*, 1309.
[7] R. K. Dubey, N. Westerveld, E. J. R. Sudhölter, F. C. Grozema, W. F. Jager, *Org. Chem. Front.* **2016**, *3*, 1481.
[8] H. Langhals, *Heterocycles* **1995**, *40*, 477.
[9] a) H. Langhals, S. Sprenger, M.-T. Brandherm, *Liebigs Ann.* **1995**, *1995*, 481; b) T. Maki, H. Hashimoto, *Bull. Chem. Soc. Jpn.* **1952**, *25*, 411.

[10] a) Y. Zhang, D. Hanifi, E. Lim, S. Chourou, S. Alvarez, A. Pun, A. Hexemer, B. Ma, Y. Liu, *Adv. Mater.* **2014**, *26*, 1223; b) J. Xie, W. Chen, Z. Wang, K. C. W. Jie, M. Liu, Q. Zhang, *Chem. Asian J.* **2017**, *12*, 868.
[11] J. Schönamsgruber, A. Hirsch, *Eur. J. Org. Chem.* **2015**, 2167.
[12] a) Y. Geerts, H. Quante, H. Platz, R. Mahrt, M. Hopmeier, A. Böhm, K. Müllen, *J. Mater. Chem.* **1998**, *8*, 2357; b) H. Quante, K. Müllen, *Angew. Chem. Int. Ed.* **1995**, *34*, 1323; *Angew. Chem.* **1995**, *107*, 1487–1489.
[13] M. Dobeneck, R. Kaur, B. Platzer, D. M. Guldi, A. Hirsch, *ChemPhotoChem* **2021**, *5*, 36.
[14] Z. Yuan, Y. Xiao, Z. Li, X. Qian, *Org. Lett.* **2009**, *11*, 2808.
[15] a) M. Könemann, T. Noe, Z. Bao, J. Hak Oh, WO2009037283 A1, **17.09**; b) L. Perrin, P. Hudhomme, *Eur. J. Org. Chem.* **2011**, 5427; c) J. Fortage, M. Séverac, C. Houarner-Rassin, Y. Pellegrin, E. Blart, F. Odobel, *J. Photochem. Photobiol. A* **2008**, *197*, 156.
[16] F. Arbeloa, P. Ojeda, I. Arbeloa, *J. Lumin.* **1989**, *44*, 105.
[17] a) Y. Wu, M. Frasconi, D. M. Gardner, P. R. McGonigal, S. T. Schneebeli, M. R. Wasielewski, J. F. Stoddart, *Angew. Chem. Int. Ed.* **2014**, *53*, 9476–9481; *Angew. Chem.* **2014**, *126*, 9630; b) J. Zhao, J. I. Wong, J. Gao, G. Li, G. Xing, H. Zhang, T. C. Sum, H. Y. Yang, Y. Zhao, S. L. Ake Kjelleberg, et al., *RSC Adv.* **2014**, *4*, 17822.
[18] > Assignments regarding the perylene-centered redox processes were based on a comparison with those reported for **3** – Table 2. Particular attention was placed on the potential difference between two consecutive processes. For the naphthalene-centered redox processes we turned to the naphthalene dimers in references 17.
[19] a) D. J. Anderson, R. McDonald, M. Cowie, *Angew. Chem. Int. Ed.* **2007**, *46*, 3741; *Angew. Chem.* **2007**, *119*, 3815–3818; b) S. F. Ralph, M. M. Sheil, L. A. Hick, R. J. Geue, A. M. Sargeson, *J. Chem. Soc. Dalton Trans.* **1996**, 4417.

Manuscript received: December 15, 2020
Accepted manuscript online: April 8, 2021
Version of record online: May 11, 2021

